Tubedown associates with cortactin and controls permeability of retinal endothelial cells to albumin

Hélène Paradis[1], Thasin Islam[1], Stephanie Tucker[1], Lidan Tao[2], Sharon Koubi[1] and Robert L. Gendron[1,*]

[1]Division of Biomedical Sciences, Department of Medicine and [2]Core Research Equipment and Instrument Training Network (CREAIT), Memorial University of Newfoundland, St John's, NL, A1B 3V6, Canada

*Author for correspondence (e-mail: rgendron@mun.ca)

Accepted 20 March 2008
Journal of Cell Science 121, 1965-1972 Published by The Company of Biologists 2008
doi:10.1242/jcs.028597

Summary

Tubedown (Narg1, Tbdn), a member of the Nat1 family of proteins, associates with the acetyltransferase Ard1 and exerts an angiostatic function in adult retinal-blood-vessel homeostasis. The purpose of the present study was to gain a better understanding of the nature of the Tbdn protein complex and how it might exert a homeostatic influence on blood vessels. Immunoprecipitation of Tbdn from endothelial cells followed by gel electrophoresis and liquid-chromatography–tandem-mass-spectrometry identified the actin-cytoskeleton-binding protein cortactin as a co-immunopurifying species. Western blotting confirmed the association between Tbdn and cortactin. Immunofluorescence confocal microscopy revealed that Tbdn colocalizes with cortactin and F-actin in cytoplasmic regions and at the cortex of cultured endothelial cells. Because cortactin is known to regulate cellular permeability through its interaction with the actin cytoskeleton, a process that is crucial for endothelial cell homeostasis, the role of Tbdn on endothelial cell permeability was examined. Knockdown of Tbdn expression in endothelial cells led to the co-suppression of Ard1 protein expression and to a significant increase in cellular permeability measured by the transit of FITC-albumin across the cellular monolayer. Furthermore, the proliferative retinal neovascularization and thickening resulting from induction of Tbdn knockdown in endothelium in transgenic mice was associated with a significant increase in extravasation or leakage of albumin from abnormal retinal blood vessels in vivo. These results provide evidence that an association occurs between Tbdn and cortactin, and that Tbdn is involved in the regulation of retinal-endothelial-cell permeability to albumin. This work implicates a functional role for Tbdn in blood-vessel permeability dynamics that are crucial for vascular homeostasis.

Key words: Tubedown, Cortactin, Actin cytoskeleton, Endothelial cells, Permeability

Introduction

Endothelial cells arise through vasculogenesis and participate in developmental angiogenesis to form the mature vascular tree (Cleaver and Melton, 2003). Homeostasis of tissues depends upon the function and behavior of endothelial cells, which participate in physiological and pathological angiogenesis, and are often specific to different vascular beds (Michiels, 2003; Cleaver and Melton, 2003; Feletou and Vanhoutte, 2006; Mehta and Malik, 2006). The intracellular proteomic networks regulating endothelial cell behavior in different vascular beds are only beginning to be defined. Our laboratory has characterized Tubedown (Tbdn, also known as Narg1 and NATH) as a protein for which high levels of expression in adults is restricted to a few specific vascular beds, including the ocular endothelium, blood vessels of regressing ovarian follicles and the choroid plexus endothelium (Gendron et al., 2000; Gendron et al., 2001; Paradis et al., 2002) (H.P., unpublished observation). Tbdn is also transiently expressed during embryogenesis in the developing vasculature and neuronal tissues, in which its regulation is associated with differentiation (Gendron et al., 2000; Sugiura et al., 2001; Sugiura et al., 2003; Arnesen et al., 2006a; Martin et al., 2007). In adults, several lines of evidence support a crucial role for Tbdn in the ocular blood vessels to maintain the homeostasis of the retina. Both the knockdown of Tbdn in animal models and the suppression of Tbdn expression in human retinal-disease specimens have been associated with increased angiogenesis and pathological neovascular retinopathies (Gendron et al., 2001; Paradis et al., 2002; Wall et al., 2004; Gendron et al., 2006).

Tbdn protein has been defined as a protein that is associated with acetyltransferase activity and is homologous to the yeast Nat1 protein, an essential subunit of the yeast N-terminal acetyltransferase NatA (Park and Szostak, 1992; Gendron et al., 2000). In yeast and mammalian cell lines, Tbdn acts in a complex with the acetyltransferase Ard1 and is involved in the regulation of a wide range of cellular processes, including cell growth and differentiation (Park and Szostak, 1992; Paradis et al., 2002; Willis et al., 2002; Sugiura et al., 2003; Gautschi et al., 2003; Kimura et al., 2003; Wang et al., 2004; Asaumi et al., 2005; Arnesen et al., 2005; Arnesen et al., 2006b). In mammalian cells, homologues for Tbdn (Nat2, 70% identity) and Ard1 (Ard2, 81% identity) have also been described (Sugiura et al., 2003; Arnesen et al., 2006a). In yeast, NatA probably mediates co-translational acetylation of nascent polypeptides at specific residues in the second position of the N-terminus upon cleavage of the initial methionine by methionine aminopeptidases (Gautschi et al., 2003; Polevoda and Sherman, 2003). Acetylation of lysine residues has also been suggested as a function of Ard1 and a wide variety of potential substrates for NatA have been reported (Polevoda and Sherman, 2003; Kimura et al., 2003; Wang et al., 2004; Geissenhoner et al., 2004; Lim et al., 2006). Recently, another protein found in association with the NatA complex is the putative acetyltransferase Nat5 (also called San in *Drosophila melanogaster*), which interacts with Nat1 in the yeast

ribosome (Gautschi et al., 2003; Williams et al., 2003; Arnesen et al., 2006c; Hou et al., 2007).

We undertook the present study to define the proteomic properties of Tbdn in endothelial cells as a step towards understanding the mechanisms by which Tbdn exerts a homeostatic influence on blood vessels. We report here that Tbdn forms a complex with the actin-binding protein cortactin and is involved in the regulation of endothelial cell permeability. Because cortactin is known to be important for endothelial permeability and migration (Daly, 2004; Kowalski et al., 2005; Mehta and Malik, 2006), our study implicates Tbdn as a participant with cortactin in endothelial cell function and homeostasis.

Results

To identify Tbdn-interacting proteins in endothelial cells, proteins co-purifying with Tbdn that was immunoprecipitated from endothelial cells by using an affinity purified anti-Tbdn antibody (C10-20) were analyzed by SDS-PAGE. The specificity of the affinity purified anti-Tbdn antibody C10-20 for immunoprecipitating Tbdn is demonstrated in Fig. 1. Immunoprecipitation of ^{35}S-labeled in-vitro-translated recombinant Tbdn protein using the anti-Tbdn C10-20 antibody was completely blocked with Tbdn C10-20-blocking peptide as compared with the negative-control peptide (Fig. 1A). SDS-PAGE and silver-staining analysis of immunoprecipitates that were obtained from endothelial cell lines by using C10-20 anti-Tbdn antibody resolved at least three major proteins of ~69, ~80 and ~95 kDa that are specific to the anti-Tbdn immunoprecipitates (Fig. 1B). In-gel tryptic digestion of the ~80-kDa bands followed by liquid-chromatography–tandem-mass-spectrometry (LC-MS/MS) analysis and Mascot searches (http://www.matrixscience.com) repeatedly identified the actin-binding protein cortactin (accession code number AAB28755) as a protein that co-immunopurifies with Tbdn. The Mows scores of

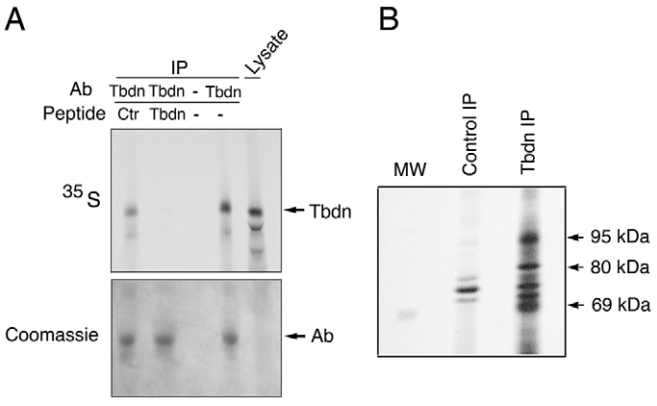

Fig. 1. Analysis of proteins in Tbdn immunoprecipitates. (A) Specificity of C10-20 antibody for Tbdn is demonstrated by immunoprecipitation (IP) of ^{35}S-labeled in-vitro-translated recombinant Tbdn protein with anti-Tbdn C10-20 antibody (Ab: Tbdn) or no antibody (Ab: –) in the absence of peptide (Peptide: –), or in the presence of control peptide (Peptide: Ctr) or Tbdn C10-20-blocking peptide (Peptide: Tbdn), followed by gel electrophoresis and Coomassie Blue staining (bottom) and autoradiography (top). Control ^{35}S-labeled in-vitro-translated Tbdn was also analyzed in parallel without immunoprecipitation (Lysate). (B) Immunoprecipitation of endothelial cell protein extracts using affinity purified anti-Tbdn antibody C10-20 (Tbdn IP) or no antibody (Control IP) followed by gel electrophoresis and silver staining. Bands of 69, 80 and 95 kDa are specific for Tbdn immunoprecipitates and are indicated by the arrows to the right of the gel.

Table 1. Cortactin peptide sequences identified in Tbdn immunoprecipitates

Sequenced amino acids	Cortactin amino acid number
SAVGFDYQGK	172-181
VDKSAVGFEYQGK	206-218
SAVGFEYQGK	209-218
TVPIEAVTSK	337-346
ANFENLAK	352-359
YGLFPANYVELR	534-545
YGLFPANYVELRQ	534-546

the Mascot identities for cortactin were as high as 295. Peptide sequences obtained from the ~80-kDa band of a representative mouse Tbdn immunoprecipitation that were sequenced by mass spectrometry and showed identity with cortactin are presented in Table 1. The actin-binding protein cortactin was matched with excellent peptide coverage (seven different sequences). Mass-spectrometry analyses of tryptic digests of immunoprecipitations performed using rabbit pre-immune serum or no antibody failed to identify cortactin. The ~95-kDa protein present in Tbdn immunoprecipitates was determined by LC-MS/MS analyses to be Tbdn (Mows scores ~800, accession code number AAH50017), whereas the ~69-kDa protein was identified as bovine albumin (Mows scores >1000, accession code number AAA51411; data not shown).

Tbdn and cortactin western blot analyses of endothelial cell protein extracts that were immunoprecipitated with C10-20 affinity purified anti-Tbdn antibody revealed the presence of Tbdn (~100 kDa)- and cortactin (~80 kDa)-reactive protein bands, respectively, in the anti-Tbdn immunoprecipitates (Fig. 2A). Reciprocal experiments in which Tbdn and cortactin western blot analyses were performed on endothelial cell protein extracts that were immunoprecipitated with an affinity purified anti-cortactin antibody (SC11408) revealed the presence of Tbdn protein (~100 kDa) and cortactin (~80 kDa), respectively, in the anti-cortactin immunoprecipitates (Fig. 2A). Tbdn was not detected in immunoprecipitates prepared using the monoclonal anti-cortactin antibody 4F11 (Fig. 2A). Detection of cortactin by western blotting of anti-Tbdn C10-20 immunoprecipitates was blocked by the presence of the Tbdn C10-20-blocking peptide in anti-Tbdn immunoprecipitates but not by the control peptide, demonstrating the specificity of the co-immunoprecipitation of cortactin in Tbdn immunoprecipitates (Fig. 2B). Cortactin was detectable by western blotting in anti-Tbdn immunoprecipitates prepared from both the IEM mouse embryonic endothelial cell line and the rhesus RF/6A choroid-retinal endothelial cell line (Fig. 2C). Whole-cell lysates prepared from IEM, RF/6A and NIH 3T3 cells were also included as positive controls in cortactin western blots (Fig. 2B,C).

The cellular distributions of Tbdn and cortactin were next examined by laser-scanning confocal immunofluorescence, double labeling with OE5 anti-Tbdn monoclonal antibody (Martin et al., 2007) and affinity purified anti-cortactin polyclonal antibody SC11408 (Fig. 3E-G). Similar immunofluorescence staining patterns were achieved with affinity purified anti-cortactin polyclonal antibody SC11408 and monoclonal anti-cortactin 4F11 (data not shown). Because cortactin colocalizes with F-actin (Daly, 2004), immunofluorescence double labeling for Tbdn and F-actin [using fluorescein isothiocyanate (FITC)-phalloidin] was also performed (Fig. 3A-C). Confocal microscopy revealed that Tbdn colocalizes with cortactin and with the F-actin cytoskeleton in cultured endothelial cells. Different slices of merged images of Tbdn- and

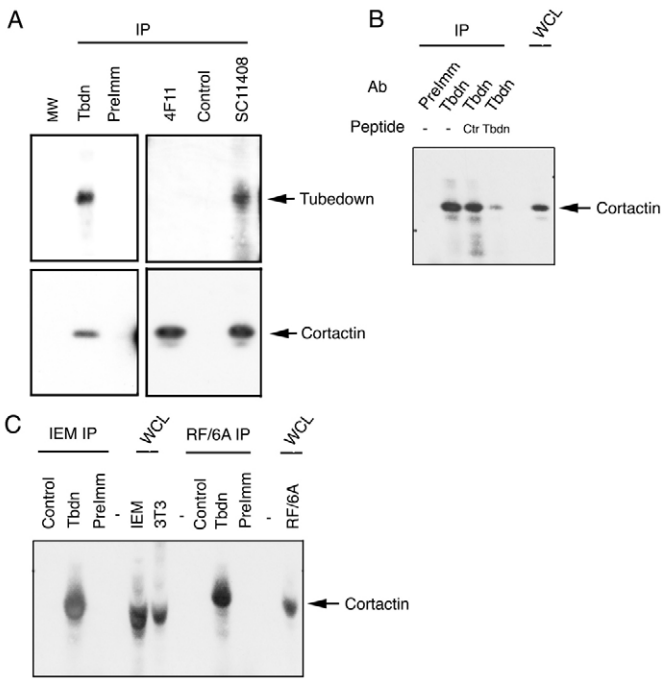

Fig. 2. Tbdn co-immunoprecipitation with cortactin. (A) The top panels show immunoprecipitation (IP) of IEM endothelial cell protein extracts using affinity purified anti-Tbdn rabbit antibody C10-20 (Tbdn), pre-immune rabbit serum (PreImm), monoclonal anti-cortactin antibody (4F11), negative-control IgG (Control) or affinity purified anti-cortactin antibody (SC11408) followed by western blotting with anti-Tbdn antibody C10-20. The blots shown in the bottom panels are the same blots as those shown in the top panels after the blots were stripped and re-probed using the anti-cortactin monoclonal antibody 4F11. Tbdn and cortactin are indicated by arrows at 100 kDa and 80 kDa, respectively. (B) Specificity of the presence of cortactin in Tbdn immunoprecipitates is demonstrated by immunoprecipitation of IEM endothelial cell protein extracts by using affinity purified anti-Tbdn antibody C10-20 (Ab: Tbdn) alone or in the presence of Tbdn C10-20-blocking peptide (Peptide: Tbdn) or control peptide (Peptide: Ctr) followed by western blotting with monoclonal anti-cortactin 4F11 antibody. PreImm, rabbit pre-immune serum. Whole-cell lysate (WCL) prepared from IEM cells was included as a positive control. An empty lane separates the IP and WCL lanes. (C) IP of protein extracts from IEM and RF/6A endothelial cells as indicated using: affinity purified anti-Tbdn antibody C10-20 (Tbdn), rabbit pre-immune serum (PreImm) or no-antibody control (Control) followed by western blotting with monoclonal anti-cortactin 4F11 antibody. Whole-cell lysates of IEM (IEM WCL), RF6A (RF/6A WCL), mouse 3T3 cells (3T3 WCL) are included as positive controls. Empty lanes are indicated (–). Representative experiments are shown.

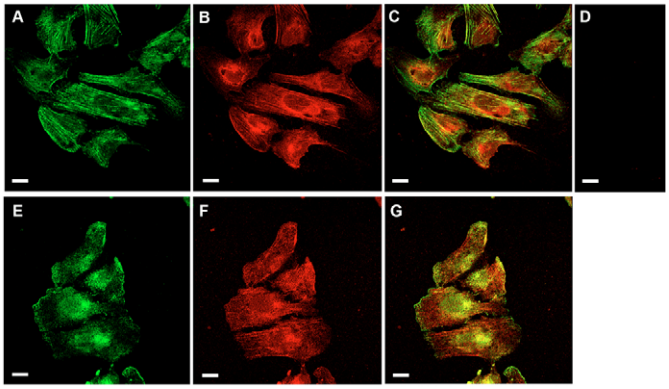

Fig. 3. Colocalization of Tbdn with F-actin and cortactin in endothelial cells. (A-C,E-G) RF/6A endothelial cells grown on glass coverslips were stained with either phalloidin for F-actin (A,C; green fluorescence) or affinity purified anti-cortactin rabbit antibody (SC11408) (E,G; green fluorescence) and then double stained with OE5 monoclonal Tbdn antibody (B,C,F,G; red fluorescence). A merged image of A and B is shown in C, and a merge of E and F is shown in G (areas of colocalization: orange/yellow). Note areas of intense colocalized staining in perinuclear areas and intense colocalization at the cortex of motile cells. (D) Merged negative control stained with negative-control antibody and vehicle control. Representative confocal microscopy of slices of cells are shown. Scale bars: 20 μm.

cortactin-stained cells, and Tbdn- and F-actin-stained cells, are shown in Fig. 3. There was an intense colocalization of Tbdn and cortactin at cytoplasmic perinuclear regions and with lamellipodia at the cell cortex (Fig. 3G). Confocal images at different levels within the cells demonstrated that there was also an intense colocalization of Tbdn and F-actin on actin fibers distributed throughout the cytoplasm of cells, which were highly visible in some of the slices (Fig. 3C). Negative controls stained with negative control antibody and vehicle only showed very minimal background staining, for which an example is shown in Fig. 3D.

Because cortactin has been implicated in regulating the dynamics of the actin cytoskeleton and plays a role in the regulation of the endothelial barrier and endothelial permeability (Weed and Parsons, 2001; Daly, 2004; Mehta and Malik, 2006), the role of Tbdn in permeability of endothelial cells was next determined. Measurements of the transit of FITC-albumin across monolayers of RF/6A endothelial cell clones in which Tbdn expression had been knocked down by stable expression of an antisense *TBDN* cDNA construct AS-*TBDN* (Paradis et al., 2002; Wall et al., 2004) were performed. The knockdown of Tbdn protein expression in RF/6A cells was associated with the suppression of Ard1 protein expression (Fig. 4A,B). The knockdown of Tbdn in RF/6A cells resulted in a significant increase in the percentage of FITC-albumin transit across the cellular monolayers compared with the RF/6A parental cell line and negative control RF/6A clones, in which Tbdn expression was not suppressed (Fig. 4C,D).

Both fluorescence microscopy of RF/6A cells incubated with FITC-albumin and measurement of intracellular uptake of FITC-albumin by RF/6A cells indicated that the permeability of endothelial cells to FITC-albumin was mediated by a transcytosis mechanism (Fig. 5). Fluorescence microscopy was consistent with the presence of FITC-albumin vesicles (green staining in Fig. 5A,D) detected inside endothelial cells; these vesicles appeared to align along the phalloidin-labeled F-actin cytoskeleton (red staining in Fig. 5B,D), but did not appear to exactly colocalize with F-actin (Fig. 5D). Similarly, Tbdn immunostaining did not colocalize with FITC-albumin (not shown). Quantitation of intracellular uptake of FITC-albumin by RF/6A endothelial cell monolayers by spectrofluorometry confirmed the fluorescence localization results and indicated an increase of intracellular FITC-albumin with time (Fig. 5E). This measurement was specific to albumin, because the fluorescence signal was competed by excess unlabeled albumin. The intracellular uptake of FITC-albumin in Tbdn-knockdown RF/6A cells was not significantly different from control cells (data not shown).

The effect of Tbdn loss on the permeability of retinal endothelial cells to albumin was next examined in mice in vivo. A previously described conditional endothelial-specific transgenic Tbdn-knockdown mouse model (Wall et al., 2004) was used for these experiments. The conditional endothelial knockdown of Tbdn in adult mice is associated with fibrovascular growth and thickening

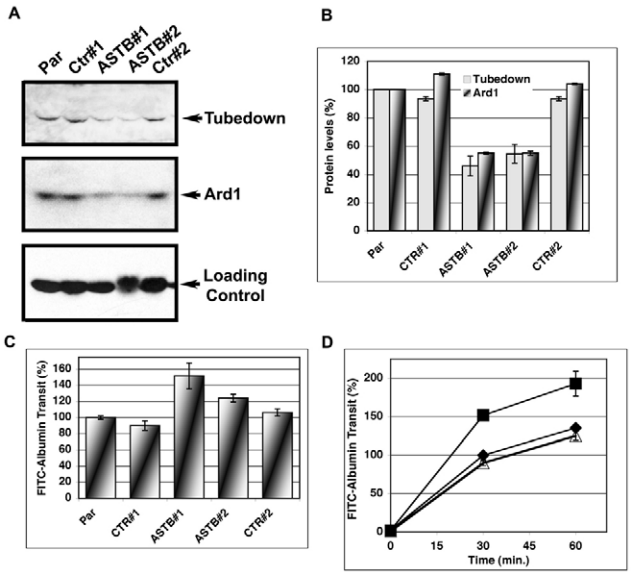

Fig. 4. Tbdn/Ard1 knockdown in endothelial cells is associated with increased cellular permeability. (A) RF/6A parental endothelial cells (Par), Tbdn-knockdown clones AS-*TBDN* (ASTB#1 and #2) and control clones (Ctr#1 and #2) analyzed by western blot for Tbdn and Ard1 expression (top and middle panels, respectively). Blots were re-probed and analyzed for tubulin as loading control (bottom panel). (A) Representative experiment; (B) the average of Tbdn and Ard1 levels ± s.e.m. are shown. (C) FITC-albumin transit across monolayers of RF/6A knocked-down for Tbdn expression (ASTB#1 and #2) or controls (Par, CTR#1 and #2) expressed as a percentage of control parental cells at 30 minutes. Significantly higher percentages of FITC-albumin transit are observed in the two AS-*TBDN* clones compared with parental cells and the two negative-control clones. (D) Time-course of FITC-albumin transit across cellular monolayers of Tbdn-knockdown RF/6A cells (ASTB#1; black square) as compared with parental cells (black diamond) and control cells (CTR#1; white triangle) expressed as percentage of arbitrary units. Data shown in C and D are expressed as mean ± s.e.m. of at least four duplicate experiments in each group.

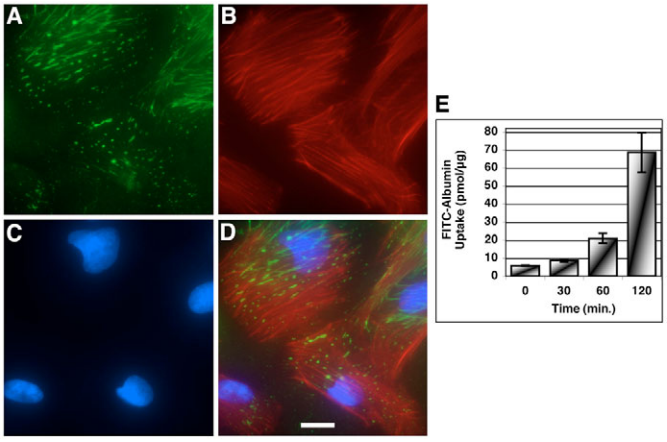

Fig. 5. Uptake measurement and localization of FITC-albumin in RF/6A endothelial cells. (A-D) Fluorescence microscopy of FITC-albumin (A,D; green fluorescence) in RF/6A endothelial cells after 60 minutes of incubation in the presence of FITC-albumin on coverslips followed by washing off excess FITC-albumin and staining for F-actin with phalloidin (B,D; red fluorescence). Cellular nuclei are highlighted by DAPI staining (C,D; blue fluorescence). The image in D represents the merge images of A-C. Scale bar: 20 µm. (E) FITC-albumin intracellular uptake by RF/6A cells as a function of time. The data shown in E are expressed as the mean of pmol per µg of protein ± s.e.m.

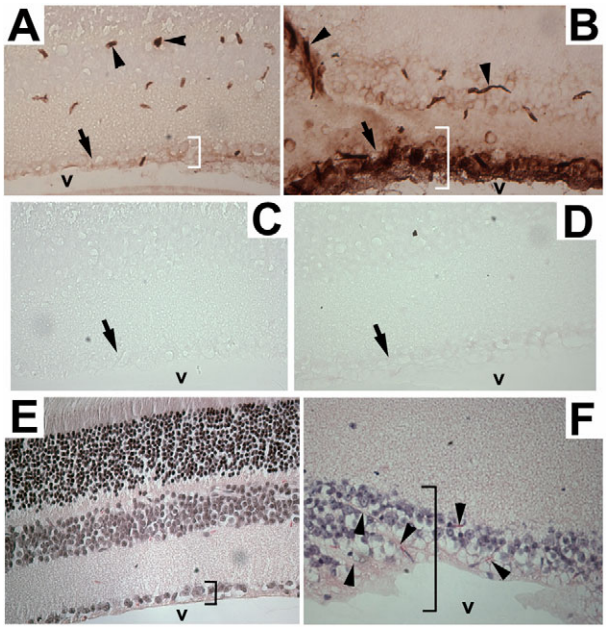

Fig. 6. Extravasation of serum albumin through the retinal-blood barrier in endothelial-specific-Tbdn-knockdown mice. Staining of retinal tissue for albumin was performed using a peroxidase-conjugated goat anti-albumin antibody, which yields a brown reaction product. Compared with control (non-induced single transgenic is shown) age-matched mice (A), endothelial-specific-Tbdn-knockdown eyes (B) showed significant leakage or extravasation of albumin (brown staining) from retinal blood vessels. Brown albumin staining is confined mainly to blood vessel lumens in control retinas (A), whereas brown albumin staining is observed in extravascular locations both in and around blood vessels and in neural retinal tissues in Tbdn-knockdown eyes (B). (C,D) Control (C) and Tbdn-knockdown (D) sections stained with negative-control horse-radish-peroxidase-conjugated goat anti-rabbit IgG at the same concentration as the anti-albumin reagent showed no staining. All images show the inner and some of the outer layers of the neural retina (most are visible in E) and are oriented with the vitreous cavity (v) of the eye at the bottom of the panel. The ganglion cell layer and inner limiting membrane, which are immediately adjacent to the vitreous (v), are arrowed near the bottom of panels A-D. (E,F) Hematoxylin and eosin staining of adjacent sections, revealing thickening of the retina and abundant abnormal blood vessels in Tbdn-knockdown retina (F) compared with control retinal tissues (E). Arrowheads in A,B,E and F point to blood vessels; brackets indicate the inner retinal layers (inner limiting membrane and ganglion cell layer). Representative images are shown. Magnification is 400×. A-D are not counterstained in order to emphasize brown albumin staining in A and B and lack of staining in C and D.

of the retinal tissues (Wall et al., 2004) (Fig. 6). Compared with control age-matched mice (Fig. 6A), the abnormal blood vessels in retinal neovascular lesions of Tbdn-knockdown mice leaked albumin, as shown by staining of extravasated albumin (Fig. 6B). The leakage was most significant from inner retinal blood vessels, which are situated in areas in which we have previously shown increases in tissue thickness and abnormal fibrovascular growth due to knockdown of Tbdn (Wall et al., 2004).

Discussion

The Tbdn protein sequence contains several tetratricopeptide (TPR) repeats, which are known to mediate protein-protein interactions (Gendron et al., 2000; Willis et al., 2002; Main et al., 2005). This information suggests that Tbdn associates specifically with other proteins. Tbdn associates with the acetyltransferase Ard1 (Sugiura et al., 2003; Arnesen et al., 2005) to form the NatA complex and

with the putative acetyltransferase Nat5 (Arnesen et al., 2006c; Hou et al., 2007), forming a complex of still-unknown function. In the present study, our results revealed that Tbdn immunoprecipitates from endothelial cell lines contain several specific co-purifying protein bands (~95, ~80, ~69 kDa) that are absent from control immunoprecipitates. Mass spectrometry analyses of these bands indicated that the ~80-kDa band is cortactin (Henzel et al., 1993; Kapp et al., 2005). The association between Tbdn and cortactin was confirmed by western blot analyses showing that cortactin was present in Tbdn immunoprecipitates, and Tbdn was identified in immunoprecipitates of cortactin performed with the SC11408 anti-cortactin antibody. Furthermore, co-immunoprecipitation of cortactin with anti-Tbdn antibody was specifically reduced by the presence of the anti-Tbdn-antibody-blocking peptide but not by a control peptide. We identified the ~95-kDa band present in anti-Tbdn immunoprecipitates as the Tbdn protein itself by LC-MS/MS and by western blotting (Fig. 2A). We noticed that Tbdn was not detected in cortactin immunoprecipitates prepared using the 4F11 anti-cortactin antibody (Fig. 2A). Because cortactin is clearly present in the 4F11 immunoprecipitates (Fig. 2A), it is possible that the 4F11 anti-cortactin antibody interferes with the association between Tbdn and cortactin. Interestingly, cortactin western blotting of endothelial cell protein extracts immunoprecipitated with anti-Tbdn antibody often revealed the presence of an anti-cortactin-reactive protein doublet (p80 and p85), similar to what was observable in whole-cell lysates of both IEM and RF/6A endothelial cells (Fig. 2B). This cortactin doublet, corresponding to changes in electrophoretic migration, has been attributed to changes in phosphorylation (Daly, 2004). The fact that both the p80 and p85 forms of cortactin are present in anti-Tbdn immunoprecipitates suggests that either Tbdn is associated with both the phosphorylated and non- or under-phosphorylated forms of cortactin, or that cortactin phosphorylation occurs in a complex containing Tbdn. Finally, our preliminary results have indicated that the complex between recombinant Tbdn and cortactin could not be reproduced in vitro, suggesting that the interaction of these two proteins is indirect or requires specific conditions that are not met in vitro.

We identified the prominent ~69-kDa band pulled down with the anti-Tbdn C10-20 antibody as bovine serum albumin by LC-MS/MS. However, this result is not surprising because this antibody was raised using a Tbdn peptide coupled to bovine serum albumin and extracts prepared from cell lines grown in media containing bovine serum albumin were used for our assays. An argument that non-specific binding to albumin might lead to artifactual pull-down of cortactin by our anti-Tbdn antibody is countered by the reciprocal co-immunoprecipitation of Tbdn by anti-cortactin antibody and by the competition of cortactin co-immunoprecipitation by the presence of the Tbdn C10-20-blocking peptide in Tbdn immunoprecipitates.

Since originally being described as a filamentous actin-binding protein and substrate of the tyrosine kinase $pp60^{src}$ in primary embryo fibroblasts, smooth muscle cells and endothelial cells (Wu and Parsons, 1993), the functional role of cortactin in regulating the dynamics of the actin-cytoskeleton assembly, cell migration, endocytosis and intracellular movement of vesicles has become well established (Weed and Parsons, 2001; Daly, 2004; Kesels and Qualmann, 2005; Kowalski et al., 2005; Mehta and Malik, 2006). The co-distribution of Tbdn and cortactin at the cell cortex and nuclear periphery is consistent with previously published reports for cortactin localization (Wu and Parsons, 1993; Cao et al., 2005) and suggests that the complex has a role in organelles surrounding the nucleus, such as the endoplasmic reticulum and Golgi complex. In agreement with this hypothesis, the yeast NatA complex has been shown to be involved in ribosome biogenesis (Gautschi et al., 2003; Polevoda et al., 2008). In addition, Tbdn colocalizes with the F-actin cytoskeleton in the cytoplasm. Studies describing the role of cortactin and the actin cytoskeleton in post-Golgi-mediated vesicle traffic and processing are only now emerging (Cao et al., 2005; Kessels and Qualmann, 2005; Egea et al., 2006). However, a single study linking vesicle transport with Tbdn protein function has been reported. Asaumi and co-workers have presented evidence that the endocytosis of β-amyloid-precursor transmembrane protein from the cell surface can be inhibited by transient overexpression of the active NatA complex, consisting of Tbdn and Ard1, in HEK293 transformed embryonic kidney cells (Asaumi et al., 2005). In addition, secretion of amyloid-β (1-40), which probably depends on the endocytosis of the β-amyloid-precursor protein, was also suppressed by overexpression of NatA, and this suppression requires the overexpression of both Ard1 and Tbdn (Asaumi et al., 2005). These results are consistent with our findings that Tbdn suppression increased the transit of FITC-labeled albumin through a cellular monolayer. Our present results show that the transit of FITC-albumin across confluent monolayers of clones of Tbdn-knockdown RF/6A endothelial cells is higher than that of control cells. Interestingly, knockdown of Tbdn in diverse cellular systems, including RF/6A endothelial cells (Fig. 4), has been associated with a reduction in Ard1 levels (Hou et al., 2007; Polevoda et al., 2008). This observation suggests that Tbdn and Ard1 together regulate FITC-albumin transit across endothelial cell monolayers.

The regulation of permeability of endothelial cells is known to be functionally important for maintaining the proper blood-retina barrier and retinal function (Mehta and Malik, 2006; Pino and Thouron, 1983; Liao and Gonzalez-Fernandez, 2004). Extravasation or leakage of serum albumin and other materials out of retinal blood vessels has been described as a marker of retinal-blood-vessel damage in humans with retinopathy (Vinores et al., 1990; Vinores et al., 1993b) and has been reported in several rodent models of breakdown of the retina-blood barrier (Vinores et al., 1999; Liu et al., 2004; Tomasek et al., 2006). The breakdown of retinal-blood-barrier function has been shown to involve changes in permeability of retinal endothelial cells (Tomasek et al., 2006), and is associated with edema and thickening of retinal tissues (Gardner et al., 2002; Sander et al., 2007). Our previous studies have shown that the loss of retinal endothelial Tbdn expression is associated with retinal fibrovascular growth and thickening, and occurs in a range of retinopathies (Gendron et al., 2001; Paradis et al., 2002; Wall et al., 2004; Gendron et al., 2006). These specific types of retinopathies are known, in some cases, to involve breakdown of the blood-retinal barrier as well as changes in retinal-endothelial-cell permeability and integrity, which are associated with extravasation of albumin (Vinores et al., 1990; Vinores et al., 1993b). In the present study, examination of endothelial-specific-Tbdn-knockdown mice revealed significant leakage of albumin from retinal blood vessels compared with control age-matched mice (Fig. 6). Overall, our results raise the possibility that increased transfer of serum proteins, such as albumin, across endothelial cells in Tbdn-suppressed blood vessels is a contributing factor to the retinal pathology present in the Tbdn-knockdown mouse model of neovascular retinopathy.

In light of the known role of cortactin in the regulation of the dynamics of the actin cytoskeleton, our findings tempt the speculation that Tbdn might participate in an acetyltransferase complex with cortactin in a range of processes involving the

regulation of the F-actin cytoskeleton in endothelial cells. Our present results on the effects of Tbdn on the transit of FITC-albumin across cellular monolayers support a model in which Tbdn is involved in at least one of these cytoskeletal-mediated structural processes in endothelial cells (Mehta and Malik, 2006). The transport of FITC-labeled albumin has been used to assess endothelial permeability in vitro (Vogel at al., 2001; Tuma and Hubbard, 2003; Irwin et al., 2005). Endothelial cell permeability and the transit of molecules across the endothelial cell barrier are dependent upon both paracellular pathways and receptor-mediated transcellular processes. The paracellular pathway involves intercellular junctions, whereas the transcellular pathway uses a vesicular system (Mehta and Malik, 2006). Previous studies have shown that albumin uses the transcellular pathway in retinal endothelial cells in vivo (Vinores et al., 1993a; Vinores et al., 1998). Our results suggest that the transit of FITC-labeled albumin across RF/6A endothelial cell monolayers occurs at least via intracellular vesicular transport (Fig. 5), as previously reported for albumin in retinal endothelial cells (Vinores et al., 1993a; Vinores et al., 1998). Our results, together with previous studies implicating Tbdn in the regulation of endocytosis (Asaumi et al., 2005), which is necessary for transcellular transport of albumin, support the notion that Tbdn is involved in the regulation of transcellular permeability. Both the para- and transcellular pathways are dependent upon the actin cytoskeleton, and cortactin probably plays a role in both processes (Tuma and Hubbard, 2003; Mehta and Malik, 2006). Cortactin has been demonstrated to interact with proteins that regulate intercellular-junction dynamics while also interacting with proteins participating in the vesicular flux of molecules across endothelial layers (Weed and Parsons, 2001; Daly, 2004; Mehta and Malik, 2006; Huang et al., 2006). Moreover, both pathways are important for vascular homeostasis (Tuma and Hubbard, 2003; Mehta and Malik, 2006). The effects of Tbdn on endothelial cell permeability are consistent with the role of Tbdn in the regulation of retinal-vascular homeostasis (Wall et al., 2004). Nevertheless, the possibility of a role for Tbdn in paracellular permeability of endothelial cells will require further studies.

Our present results provide evidence that Tbdn interacts with the actin-binding protein cortactin and provide new insight into how Tbdn affects retinal-vascular function. Whether cortactin functions specifically with Tbdn in regulating retinal-endothelial-cell permeability is currently under investigation by our laboratory.

Materials and Methods

Cell culture

The IEM mouse embryonic endothelial and RF/6A rhesus macaque choroid-retina endothelial cell lines were grown as previously described (Lou and Hu, 1987; Gendron et al., 1996; Paradis and Gendron, 2000; Gendron et al., 2001). RF/6A endothelial cell clones in which Tbdn expression had been suppressed by stable expression of the antisense *TBDN* cDNA construct AS-*TBDN* and negative control RF/6A clones in which Tbdn expression was not suppressed have been described previously (Paradis et al., 2002).

Animals

Choroid-retinal endothelial Tbdn expression was conditionally knocked down in *TIE2/rtTA/Enh-TRE/ASTBDN* bi-transgenic mice (Wall et al., 2004) for 10 weeks during adulthood (young adult to middle-age adult). Conditional knockdown of Tbdn in endothelial cells was facilitated by feeding the mice with commercially prepared mouse chow containing doxycline (Dox; 600 mg/kg; Bio-Serv, New Jersey), whereas control age-matched mice were fed with a regular diet not containing Dox. Additional controls included age-matched single transgenic mice (*TIE2/rtTA/Enh* mice or *TRE/ASTBDN* mice) fed with Dox diet for the same length of time. Eyes from sacrificed Dox-fed double transgenic and control mice were analyzed by histology as described previously (Wall et al., 2004) to determine the extent and progression of choroid-retinal pathology. The care and use of animals in this study followed the guidelines set by the Canadian Council on Animal Care and were approved by the Institutional Animal Care Committee of Memorial University of Newfoundland.

Antibodies

A polyclonal anti-Tbdn antibody (C10-20) was raised in rabbits with a peptide corresponding to the amino acid sequence 10-20 of mouse Tbdn-1 (EAWTKYPRGL) (Gendron et al., 2000) to which a cysteine residue was added to the amino terminus to facilitate coupling to bovine serum albumin (Pierce, Rockford, IL). To improve the specificity of the rabbit anti-Tbdn antibody, the anti-Tbdn C10-20 antiserum was affinity purified with the C10-20 Tbdn peptide (Covance, Denver, PA) that was used to raise the antibody. The specificity of the affinity purified anti-Tbdn antibody C10-20 for immunoprecipitating Tbdn is demonstrated in Fig. 1. A second polyclonal anti-Tbdn rabbit antibody was raised against a peptide corresponding to the amino acid sequence 755-766 (LKRNSDSLPHRL) of human Tbdn100 (Fluge et al., 2002) to which a cysteine residue was added to the amino terminus to facilitate coupling to keyhole limpet hemocyanin (KLH; Pierce, Rockford, IL). Specificity of this antiserum was demonstrated by its ability to immunoprecipitate recombinant Tbdn and by competition of the western blot signal for Tbdn with the Tbdn blocking peptide C755-766 (data not shown).

Monoclonal mouse anti-Tbdn antibody OE5 was derived as described previously (Martin et al., 2007) and its specificity was validated by confirming that it specifically recognizes recombinant Tbdn protein.

Other antibodies used in this study include mouse monoclonal anti-cortactin 4F11 (Upstate Biotechnology, Lake Placid, NY), affinity purified rabbit polyclonal anti-cortactin antibody SC11408 (Santa Cruz Biotechnology, Santa Cruz, CA), affinity purified goat anti-Ard1 antibody (Santa Cruz Biotechnology, Santa Cruz, CA), α-tubulin mouse monoclonal antibody (Sigma, St Louis, MO) and negative-control isotype-match mouse IgG1 and IgG2a (Dako, Glostrup, DK). We also used an affinity purified horse radish peroxidase (HRP)-conjugated goat anti-albumin IgG (GeneTex, San Antonio, TX) and an affinity purified HRP-conjugated goat anti-rabbit IgG antibody reagent (Promega, Madison, WI) as a negative isotype control for the albumin staining.

Protein preparations and immunoprecipitations

Protein extraction was performed essentially as described previously (Gendron et al., 2000). Cellular monolayers were washed twice with 25 mM Tris-HCl pH 7.6, 150 mM NaCl, harvested and suspended in a cell lysis buffer (50 mM Tris-HCl pH 7.6, 150 mM NaCl and 0.5% Brij 96) supplemented with protease inhibitors (1 mM phenylmethylsulfonyl fluoride, 0.3 U/ml aprotinin and 10 μg/ml leupeptin) and phosphatase inhibitors (1 mM sodium orthovanadate, 25 mM sodium fluoride and 10 mM β-glycerophosphate). Lysates were clarified by centrifugation and proteins were quantified. ^{35}S-labeled in-vitro-translated recombinant Tbdn was produced using the TNT Quick Coupled Transcription/Translation Systems kit (Promega, Madison, WI) as described previously (Wall et al., 2004).

For immunoprecipitations, cell lysates or in-vitro-translated recombinant Tbdn protein were incubated for 4 hours or overnight at 4°C with affinity purified anti-Tbdn rabbit antibody C10-20, rabbit pre-immune serum, negative control IgG or no antibody control. Immunoprecipitates were also performed using monoclonal anti-cortactin 4F11 antibody (Upstate Biotechnology, Lake Placid, NY) or affinity purified polyclonal anti-cortactin SC11408 antibody (Santa Cruz Biotechnology, Santa Cruz, CA). Immune complexes were purified with protein-G–Sepharose beads (Amersham Biosciences, Piscataway, NJ). For blocking-peptide experiments, immunoprecipitation was performed using the anti-Tbdn antibody C10-20 or no antibody in the absence or presence of 200 μM of a control peptide (PDASFPLSLMSTDKHTNFF) or 200 μM of Tbdn C10-20-blocking peptide (CEAWTKYPRGL) and 500 μM of bacitracin as protease inhibitor.

Immunoprecipitates were analyzed by SDS-PAGE. Gels were either processed for western blot analyses or stained with silver nitrate, or alternatively with Coomassie Blue for processing for mass spectrometry, as described below, or autoradiography for detection of ^{35}S-labeled proteins described above.

For silver staining, gels were fixed in a solution containing methanol:glacial acetic acid:water (45:5:50) for 45 minutes followed by two 10-minute water washes and 3 minutes in 0.02% sodium thiosulfate. Gels were next rinsed twice in water and incubated for 25 minutes in 0.1% silver nitrate. After a rinse with water, proteins were visualized with 2.5% sodium carbonate/0.02% formaldehyde. The reaction was stopped with 1% glacial acetic acid.

Western blot analyses

Western blots were performed by standard procedures using ECL Plus chemiluminescence detection reagent (Amersham Biosciences, Piscataway, NJ) for detection of cortactin with mouse monoclonal anti-cortactin 4F11 and for detection of Tbdn with rabbit anti-Tbdn C10-20 or C755-766 antibody. Western blots were stripped and re-probed with α-tubulin mouse monoclonal antibody (Sigma, St Louis, MO) to determine loading equivalency. Densitometry analyses were conducted using the Kodak Gel Logic 200 imaging system (Eastman Kodak Company, Rochester, NY) and intensities of the expressed bands were analyzed using Kodak Molecular imaging software (Version 4.0, Eastman Kodak Company, Rochester, NY).

LC-MS/MS and protein identification

The procedure for LC-MS/MS analyses was similar to previously published methodology (Alvarez et al., 2006). SDS-PAGE were fixed in 40% methanol, 10% acetic acid for 30 minutes and stained for 2 hours with Coomassie Blue G-250 (Bio-Rad Laboratories, Hercules, CA). Protein bands of interest were excised, washed three times for 10 minutes each with water followed by complete dehydration in acetonitrile (ACN) and then dried. Gel pieces were rehydrated and proteins reduced with dithiothreitol in ammonium bicarbonate buffer followed by treatment with 10 mM iodoacetamine for 30 minutes at 22°C. Gel pieces were washed with water and ACN and dried. Proteins were digested with 5 ng/μl of a modified trypsin (Promega, Madison, WI) solution overnight at 37°C. Peptides were extracted with 50% ACN/0.15% trifluoroacetic acid (TFA) followed by volume reduction using a Speedvac. The protein digests were diluted in 0.1% formic acid (FA), loaded onto a C18 precolumn and separated on a nanoflow analytical C18 HPLC column (75 μm i.d., Dionex Canada, Oakville, ON) at 180 nl/minute using a linear gradient of 0% to 60% of 0.08% FA/0.008% TFA/98% ACN (buffer A) and 100% to 40% of 0.1% FA/0.01% TFA/2% acetonitrile (buffer B), which was applied for 62 minutes. A Qstar XL hybrid quadrupole TOF MS/MS with a nanoelectrospray source (Applied Biosystems, Bellerica, MA) was used for peptide sequence analysis. The nanoelectrospray was generated from a 10 μm i.d. PicoTip needle (New Objectives, Woburn, MA). TOF MS spectra and MS/MS spectra of doubly and triply charged precursor ion were acquired using Analyst QS software. The peptide tandem MS/MS spectra were used for database searches with Mascot software (http://matrixscience.com) installed on a local server. Peptide tolerance and MS/MS tolerance was set at 0.2 Da for data searches with no imposed limit for species specificity or molecular weights. Additional search criteria included carbamidomethyl modification of cysteine residue, oxidation of methionine and allowing 1 missed trypsin cleavage. All searches were made against the NCBI nr protein database.

Immunofluorescence staining, confocal microscopy and immunohistochemistry

Cells were grown overnight on glass coverslips, fixed in phosphate buffered saline (PBS) containing 4% paraformaldehyde for 10 minutes and permeabilized with PBS containing 0.2% Triton X-100 (PBT) for 15 minutes. For cortactin labeling, cells were blocked for 1 hour in 2% goat serum in PBS and were incubated with 4 μg/ml of affinity purified rabbit polyclonal anti-cortactin antibody SC11408 (Santa Cruz Biotechnology, Santa Cruz, CA) in PBT for 2 hours followed by 1 hour with FITC-conjugated anti-rabbit IgG (Sigma, St Louis, MO). To localize F-actin, cells were incubated with 2.5 μM FITC-conjugated phalloidin (Sigma, St Louis, MO) in 1% dimethylsulfoxide (DMSO) for 40 minutes. For double labeling, cells were further incubated for 1 hour in 6% low-fat dried powdered milk in PBT followed by 5 μg/ml of OE5 anti-Tbdn mouse monoclonal antibody overnight in 3% milk/PBT. Cells were next incubated for 1 hour with rhodamine-conjugated anti-mouse IgG (Jackson ImmunoResearch Laboratories, West Grove, PA). Negative controls for cortactin, Tbdn and F-actin stainings were respectively, no antibody, isotype-match IgG2a negative-control antibody and vehicle alone (1% DMSO). Cells were mounted on glass slides with Vectashield aqueous mounting medium containing DAPI (Vector Laboratories, Burlingame, CA) and visualized under a laser-scanning confocal microscope (Olympus, Center Valley, PA). Resulting digital images were further analyzed using Adobe Photoshop.

Paraffin sections from eyes from Dox-fed endothelial-specific-Tbdn-knockdown mice and control mice sacrificed at appropriate time points were processed for immunostaining as described previously (Wall et al., 2004) and analyzed by albumin immunohistochemistry to assess retinal albumin expression/localization. Mouse tissues were fixed in 4% paraformaldehyde, embedded in paraffin and processed for immunohistochemistry, as previously described (Paradis et al., 2002). Briefly, sections were de-waxed in xylene and rehydrated in graded alcohols. For melanin bleaching, sections were incubated with 0.25% $KMnO_4$ for 5 minutes, rinsed with 10 mM Tris-HCl pH 7.6, 150 mM NaCl (TBS), followed by a 5-minute incubation in 1% oxalic acid and three 5-minute washes with TBS. Endogenous peroxidases were blocked in 0.3% H_2O_2 for 10 minutes followed by post-fixation with 4% paraformaldehyde for 10 minutes. Sections were incubated for 1 hour with 6% fat-free skimmed powdered milk in TBS containing 0.05% Tween 20 (TBST) for blocking non-specific binding sites followed by incubation with goat anti-albumin HRP-conjugated antibody in 3% powdered milk/TBST overnight at room temperature. Control and Tbdn-knockdown sections were also stained with HRP-conjugated goat anti-rabbit IgG at the same concentration as the anti-albumin antibody as a negative control for the albumin staining. The peroxidase activity was detected using NovaRed substrate kit (Vector Laboratories, Burlingame, CA) according to the manufacturer's instructions. Sections were then air-dried and mounted in Permount (Fisher Scientific, Pittsburg, PA). Adjacent sections were stained with hematoxylin and eosin in order to enable assessment of tissue integrity and pathology.

Cellular permeability assay analyses

For FITC-albumin transit assays, RF/6A cells [parental cells, stable AS-*TBDN* clones and control clones (Paradis et al., 2002)] were seeded onto 1%-gelatin-coated polystyrene filter inserts (Costar Transwell, no. 3470, 6.5-mm diameter, 0.4-μm pore size; Sigma, St Louis, MO) in Dulbecco's modified Eagle media (DMEM) (Invitrogen) supplemented with 2 mM glutamine plus 10% FBS and 50 μM of nonessential amino acids at a density of 30,000 cells/insert (0.3×10^6 cells/ml). The cells were grown to confluence on the Transwell inserts over 24 hours. The integrity of the cellular monolayer was evaluated for confluence by phase-contrast light microscopy and photographed. Cells were then washed three times in DMEM and the inserts were transferred into new 24-well plates containing DMEM and incubated for 2 hours. FITC-labeled albumin (Sigma A9771, Sigma, St Louis, MO) suspended in DMEM was added to the endothelial cell monolayers to achieve a final FITC-albumin concentration of 100 μM. Transit rate of FITC-albumin across the monolayer was assessed by measuring the increase in FITC-albumin in the lower well at different time points from 0 to 60 minutes (Irwin et al., 2005). FITC-albumin was quantified against a standard curve of FITC-albumin using a FLUOstar Optima spectrofluorometer (BMG Labtechnologies) at an excitation wavelength of 485 nm and an emission wavelength of 520 nm.

For visualizing FITC-albumin inside cells, RF/6A parental cells were plated on coverslips, washed with DMEM and incubated for 2 hours. Cell monolayers were next incubated with FITC-albumin for 0-120 minutes as described above. At the end of incubations, cells were processed for phalloidin staining as described above and photographed under fluorescent microscope.

Intracellular FITC-albumin content was measured using a procedure adapted from Takano et al. (Takano et al., 2002). RF/6A cells were plated at 0.75×10^6 cells/ml on 35-mm culture dishes. The cells were grown to confluence over 24 hours. Cells were then washed three times in DMEM and incubated for 2 hours. 10 μM FITC-albumin was added to the plates and cells were incubated for 0-120 minutes at 37°C. After each incubation period, the dishes were rinsed rapidly three times with 1 ml of ice-cold PBS. The cells were then scraped in ice-cold PBS and centrifuged at 4°C. Cells were lysed with PBS containing 0.1% Triton X-100, and the fluorescence and protein concentration of the homogenates was measured as described above.

Statistical analyses

Values were expressed as the mean percentage of the control or mean of pmol per μg of protein, as indicated, ± s.e.m. Quantitative analyses were compared using the two-tailed Student's *t*-test with a Microsoft Excel program. The data was considered to be statistically significant if the *P*-value was less than or equal to 0.05.

We thank Gary Paterno, Laura Gillespie, Ewa Miskiewicz and Catherine Barry of Memorial University of Newfoundland for expert assistance with antibodies. This work was supported by Canadian Institutes of Health Research and Foundation Fighting Blindness Canada Operating Grants to R.L.G. and H.P., and by a Memorial University Graduate Studentship and an Alfred Burness Graduate Student Award to T.I. Instrumentation and infrastructure essential for this project was supported by Awards from Canada Foundation for Innovation New Opportunities Fund (project number 7411) and Opportunities Fund (project number 7972).

References

Alvarez, S., Goodger, J. Q., Marsh, E. L., Chen, S., Asirvatham, V. S. and Schachtman, D. P. (2006). Characterization of the maize xylem sap proteome. *J. Proteome Res.* **5**, 963-972.

Arnesen, T., Anderson, D., Baldersheim, C., Lanotte, M., Varhaug, J. E. and Lillehaug, J. R. (2005). Identification and characterization of the human ARD1-NATH protein acetyltransferase complex. *Biochem. J.* **386**, 433-443.

Arnesen, T., Betts, M. J., Pendino, F., Liberles, D. A., Anderson, D., Caro, J., Kong, X., Varhaug, J. E. and Lillehaug, J. R. (2006a). Characterization of hARD2, a processed hARD1 gene duplicate, encoding a human protein N-alpha-acetyltransferase. *BMC Biochem.* **7**, 13.

Arnesen, T., Gromyko, D., Pendino, F., Ryningen, A., Varhaug, J. E. and Lillehaug, J. R. (2006b). Induction of apoptosis in human cells by RNAi-mediated knockdown of hARD1 and NATH, components of the protein N-alpha-acetyltransferase complex. *Oncogene* **25**, 4350-4360.

Arnesen, T., Anderson, D., Torsvik, J., Halseth, H. B., Varhaug, J. E. and Lillehaug, J. R. (2006c). Cloning and characterization of hNAT5/hSAN: an evolutionarily conserved component of the NatA protein N-alpha-acetyltransferase complex. *Gene* **371**, 291-295.

Asaumi, M., Iijima, K., Sumioka, A., Iijima-Ando, K., Kirino, Y., Nakaya, T. and Suzuki, T. (2005). Interaction of N-terminal acetyltransferase with the cytoplasmic domain of beta-amyloid precursor protein and its effect on A beta secretion. *J. Biochem.* **137**, 147-155.

Cao, H., Weller, S., Orth, J. D., Chen, J., Huang, B., Chen, J. L., Stamnes, M. and McNiven, M. A. (2005). Actin and Arf1-dependent recruitment of a cortactin-dynamin complex to the Golgi regulates post-Golgi transport. *Nat. Cell Biol.* **7**, 483-492.

Cleaver, O. and Melton, D. A. (2003). Endothelial signaling during development. *Nat. Med.* **9**, 661-668.

Daly, R. J. (2004). Cortactin signalling and dynamic actin networks. *Biochem. J.* **382**, 13-25.

Egea, G., Lazaro-Dieguez, F. and Vilella, M. (2006). Actin dynamics at the Golgi complex in mammalian cells. *Curr. Opin. Cell Biol.* **18**, 168-178.

Feletou, M. and Vanhoutte, P. M. (2006). Endothelial dysfunction: a multifaceted disorder. *Am. J. Physiol. Heart Circ. Physiol.* **291**, H985-H1002.

Fluge, O., Bruland, O., Akslen, L. A., Varhaug, J. E. and Lillehaug, J. R. (2002). NATH, a novel gene overexpressed in papillary thyroid carcinomas. *Oncogene* **21**, 5056-5068.

Gardner, T. W., Antonetti, D. A., Barber, A. J., LaNoue, K. F. and Levison, S. W. (2002). Diabetic retinopathy: more than meets the eye. *Surv. Ophthalmol*. **47** Suppl. 2, S253-S262.

Gautschi, M., Just, S., Mun, A., Ross, S., Rucknagel, P., Dubaquie, Y., Ehrenhofer-Murray, A. and Rospert, S. (2003). The yeast N(alpha)-acetyltransferase NatA is quantitatively anchored to the ribosome and interacts with nascent polypeptides. *Mol. Cell. Biol.* **23**, 7403-7414.

Geissenhoner, A., Weise, C. and Ehrenhofer-Murray, A. E. (2004). Dependence of ORC silencing function on NatA-mediated Nalpha acetylation in Saccharomyces cerevisiae. *Mol. Cell. Biol.* **24**, 10300-10312.

Gendron, R. L., Tsai, F. Y., Paradis, H. and Arceci, R. J. (1996). Induction of embryonic vasculogenesis by bFGF and LIF in vitro and in vivo. *Dev. Biol.* **177**, 332-346.

Gendron, R. L., Adams, L. C. and Paradis, H. (2000). Tubedown-1, a novel acetyltransferase associated with blood vessel development. *Dev. Dyn.* **218**, 300-315.

Gendron, R. L., Good, W. V., Adams, L. C. and Paradis, H. (2001). Expression of tubedown-1 is suppressed in retinal neovascularization of proliferative diabetic retinopathy. *Invest. Opthalmol. Vis. Sci.* **42**, 3000-3007.

Gendron, R. L., Good, W. V., Miskiewicz, E., Tucker, S., Phelps, D. L. and Paradis, H. (2006). Tubedown-1 (Tbdn-1) suppression in oxygen-induced retinopathy and in retinopathy of prematurity. *Mol. Vis*. **12**, 108-116.

Henzel, W. J., Billeci, T. M., Stults, J. T., Wong, S. C., Grimley, C. and Watanabe, C. (1993). Identifying proteins from two-dimensional gels by molecular mass searching of peptide fragments in protein sequence databases. *Proc. Natl. Acad. Sci. USA* **90**, 5011-5015.

Hou, F., Chu, C. W., Kong, X., Yokomori, K. and Zou, H. (2007). The acetyltransferase activity of San stabilizes the mitotic cohesin at the centromeres in a shugoshin-independent manner. *J. Cell Biol.* **21**, 587-597.

Huang, R., Cao, G. J., Guo, H., Kordowska, J. and Wang, C.-L. A. (2006). Direct interaction between caldesmon and cortactin. *Arch. Biochem. Biophys.* **456**, 175-182.

Irwin, D. C., Tissot van Patot, M. C., Tucker, A. and Bowen, R. (2005). Direct ANP inhibition of hypoxia-induced inflammatory pathways in pulmonary microvascular and macrovascular endothelial monolayers. *Am. J. Physiol. Lung Cell. Mol. Physiol.* **288**, 849-859.

Kapp, E. A., Schutz, F., Connolly, L. M., Chakel, J. A., Meza, J. E., Miller, C. A., Fenyo, D., Eng, J. K., Adkins, J. N., Omenn, G. S. et al. (2005). An evaluation, comparison, and accurate benchmarking of several publicly available MS/MS search algorithms: sensitivity and specificity analysis. *Proteomics* **5**, 3475-3490.

Kessels, M. M. and Qualmann, B. (2005). Extending the court for cortactin: from the cortex to the Golgi. *Nat. Cell Biol.* **7**, 448-449.

Kimura, Y., Saeki, Y., Yokosawa, H., Polevoda, B., Sherman, F. and Hirano, H. (2003). N-Terminal modifications of the 19S regulatory particle subunits of the yeast proteasome. *Arch. Biochem. Biophys*. **409**, 341-348.

Kowalski, J. R., Egile, C., Gil, S., Snapper, S. B., Li, R. and Thomas, S. M. (2005). Cortactin regulates cell migration through activation of N-WASP. *J. Cell Sci.* **118**, 79-87.

Liao, R. and Gonzalez-Fernandez, F. (2004). Albumin is not present in the murine interphotoreceptor matrix, or in that of transgenic mice lacking IRBP. *Mol. Vis*. **10**, 1038-1046.

Lim, J. H., Park, W. and Chun, Y. S. (2006). Human arrest defective 1 acetylates and activates beta-catenin, promoting lung cancer cell proliferation. *Cancer Res*. **66**, 10677-10682.

Liu, H., Demetriades, A. M., Xiao, W. H., Campochiaro, P. A. and Vinores, S. A. (2004). Mouse model of post-surgical breakdown of the blood-retinal barrier. *Curr. Eye Res*. **28**, 42142-42146.

Lou, D. A. and Hu, F. N. (1987). Specific antigen and organelle expression of a long-term rhesus endothelial cell line. *In Vitro Cell. Dev. Biol.* **23**, 75-85.

Main, E. R., Stott, K., Jackson, S. E. and Regan, L. (2005). Local and long-range stability in tandemly arrayed tetratricopeptide repeats. *Proc. Natl. Acad. Sci. USA* **102**, 5721-5726.

Martin, D. T., Gendron, R. L., Jarzembowski, J. A., Perry, A., Collins, M. H., Pushpanathan, C., Miskiewicz, E., Castle, V. P. and Paradis, H. (2007). Tubedown expression correlates with the differentiation status and aggressiveness of neuroblastic tumors. *Clin. Cancer Res*. **13**, 1480-1487.

Mehta, D. and Malik, A. B. (2006). Signaling mechanisms regulating endothelial permeability. *Physiol. Rev*. **86**, 279-367.

Michiels, C. (2003). Endothelial cell functions. *J. Cell. Physiol.* **196**, 430-443.

Paradis, H. and Gendron, R. L. (2000). LIF tranduces contradictory signals on capillary outgrowth through induction of Stat3 and $^{P41/43}$MAP kinase. *J. Cell Sci*. **113**, 4331-4339.

Paradis, H., Liu, C. Y., Saika, S., Azhar, M., Doetschman, T., Good, W. V., Nayak, R., Laver, N., Kao, C. W., Kao, W. W. et al. (2002). Tubedown-1 in TGF-b2 mediated remodeling of the developing vitreal vasculature in vivo and regulation of capillary outgrowth in vitro. *Dev. Biol*. **249**, 140-155.

Park, E. C. and Szostak, J. W. (1992). ARD1 and NAT1 proteins form a complex that has N terminal acetyltransferase activity. *EMBO J.* **11**, 2087-2093.

Pino, R. M. and Thouron, C. L. (1983). Vascular permeability in the rat eye to endogenous albumin and immunoglobulin G (IgG) examined by immunohistochemical methods. *J. Histochem. Cytochem*. **31**, 411-416.

Polevoda, B. and Sherman, F. (2003). N-terminal acetyltransferases and sequence requirements for N-terminal acetylation of eukaryotic proteins. *J. Mol. Biol.* **325**, 595-622.

Polevoda, B., Brown, S., Cardillo, T. S., Rigby, S. and Sherman, F. (2008). Yeast N(alpha)-terminal acetyltransferases are associated with ribosomes. *J. Cell. Biochem.* **103**, 492-508.

Sander, B., Thornit, D. N., Colmorn, L., Strøm, C., Girach, A., Hubbard, L. D., Lund-Andersen, H. and Larsen, M. (2007). Progression of diabetic macular edema: correlation with blood retinal barrier permeability, retinal thickness, and retinal vessel diameter. *Invest. Ophthalmol. Vis. Sci.* **48**, 3983-3987.

Sugiura, N., Patel, R. G. and Corriveau, R. A. (2001). N-methyl-D-aspartate receptors regulate a group of transiently expressed genes in the developing brain. *J. Biol. Chem.* **276**, 14257-14263.

Sugiura, N., Adams, S. M. and Corriveau, R. A. (2003). An evolutionarily conserved N-terminal acetyltransferase complex associated with neuronal development. *J. Biol. Chem.* **278**, 40113-40120.

Takano, M., Nakanishi, N., Kitahara, Y., Sasaki, Y., Murakami, T. and Nagai, J. (2002). Cisplatin-induced inhibition of receptor-mediated endocytosis of protein in the kidney. *Kidney Int.* **62**, 1707-1717.

Tomasek, J. J., Haaksma, C. J., Schwartz, R. J., Vuong, D. T., Zhang, S. X., Ash, J. D., Ma, J. X. and Al-Ubaidi, M. R. (2006). Deletion of smooth muscle alpha-actin alters blood-retina barrier permeability and retinal function. *Invest. Ophthalmol. Vis. Sci*. **47**, 2693-2700.

Tuma, P. L. and Hubbard, A. L. (2003). Transcytosis: crossing cellular barriers. *Physiol. Rev.* **83**, 871-932.

Vinores, S. A., Campochiaro, P. A., Lee, A., McGehee, R., Gadegbeku, C. and Green, W. R. (1990). Localization of blood-retinal barrier breakdown in human pathologic specimens by immunohistochemical staining for albumin. *Lab. Invest*. **62**, 742-750.

Vinores, S. A., Van Niel, E., Swerdloff, J. L. and Campochiaro, P. A. (1993a). Electron microscopic immunocytochemical evidence for the mechanism of blood-retinal barrier breakdown in galactosemic rats and its association with aldose reductase expression and inhibition. *Exp. Eye Res*. **57**, 723-735.

Vinores, S. A., Van Niel, E., Swerdloff, J. L. and Campochiaro, P. A. (1993b). Electron microscopic immunocytochemical demonstration of blood-retinal barrier breakdown in human diabetics and its association with aldose reductase in retinal vascular endothelium and retinal pigment epithelium. *Histochem. J*. **25**, 648-663.

Vinores, S. A., Derevjanik, N. L., Mahlow, J., Berkowitz, B. A. and Wilson, C. A. (1998). Electron microscopic evidence for the mechanism of blood-retinal barrier breakdown in diabetic rabbits: comparison with magnetic resonance imaging. *Pathol. Res. Pract.* **194**, 497-505.

Vinores, S. A., Derevjanik, N. L., Ozaki, H., Okamoto, N. and Campochiaro, P. A. (1999). Cellular mechanisms of blood-retinal barrier dysfunction in macular edema. *Doc. Ophthalmol*. **97**, 217-228.

Vogel, S. M., Easington, C. R., Minshall, R. D., Niles, W. D., Tiruppathi, C., Hollenberg, S. M., Parrillo, J. E. and Malik, A. B. (2001). Evidence of transcellular permeability pathway in microvessels. *Microvasc. Res.* **61**, 87-101.

Wall, D. S., Gendron, R. L., Good, W. V., Miskiewicz, E., Woodland, M., Leblanc, K. and Paradis, H. (2004). Conditional knockdown of tubedown-1 in endothelial cells leads to neovascular retinopathy. *Invest. Ophthalmol. Vis. Sci.* **45**, 3704-3712.

Wang, X., Connelly, J. J., Wang, C. L. and Sternglanz, R. (2004). Importance of the Sir3 N-terminus and its acetylation for yeast transcriptional silencing. *Genetics* **168**, 547-551.

Weed, S. A. and Parsons, J. T. (2001). Cortactin: coupling membrane dynamics to cortical actin assembly. *Oncogene* **20**, 6418-6434.

Williams, B. C., Garrett-Engele, C. M., Li, Z., Williams, E. V., Rosenman, E. D. and Goldberg, M. L. (2003). Two putative acetyltransferases, san and deco, are required for establishing sister chromatid cohesion in Drosophila. *Curr. Biol.* **13**, 2025-2036.

Willis, D. M., Loewy, A. P., Charlton-Kachigian, N., Shao, J. S., Ornitz, D. M. and Towler, D. A. (2002). Regulation of osteocalcin gene expression by a novel Ku antigen transcription factor complex. *J. Biol. Chem.* **277**, 37280-37291.

Wu, H. and Parsons, J. T. (1993). Cortactin, an 80/85-kilodalton pp60src substrate, is a filamentous actin-binding protein enriched in the cell cortex. *J. Cell Biol.* **120**, 1417-1426.